Selective Microsphere Adsorption and Metallization on Photopatterned Polycation Single-layered Adsorption Films

M. NAKAGAWA

[Award Accounts: SPSJ Hitachi Chemical Award (2005)]
Vol. 38, No. 6, pp 507–515 (2006)

Multivalent cationic molecular and macromolecular adsorbates with plural pyridinium groups were adsorbed irreversibly on a substrate surface taking a negative charge, giving their single-layered adsorption film showing high desorption resistance toward deionized water. Positive- or negative-type micropatterning, consisting of the surface adsorption, the pattern exposure, and the development, could be carried out on the basis of the promotion or suppression of desorption controlled by photochemical means. The photopatterned adsorption films were available as templates for selective microsphere adsorption and metallization by electroless deposition.

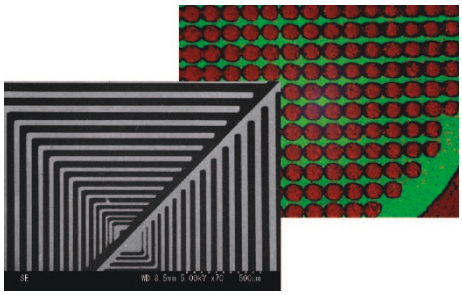

Living Radical Polymerization of Methyl Methacrylate with a Rhodium(III) Complex–Organic Halide System in Dimethyl Sulfoxide

N. KAMEDA

[Regular Article]
Vol. 38, No. 6, pp 516–522 (2006)

The rhodium(III) complex $RhH_2(Ph_2N_3)(PPh_3)_2$ in conjunction with CCl_4 was successfully used in the living radical polymerization of MMA in DMSO. For this system, polymerization followed first-order kinetics with respect to the monomer, and the number-average molecular weight (M_n) of the polymers produced increased in direct proportion to the monomer conversion. On addition of further monomer, the M_n of the polymer continued to increase in direct proportion to the monomer conversion. The polymers obtained had broad molecular-weight distributions.

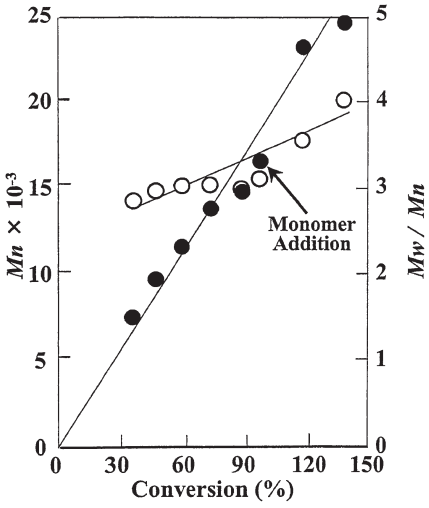

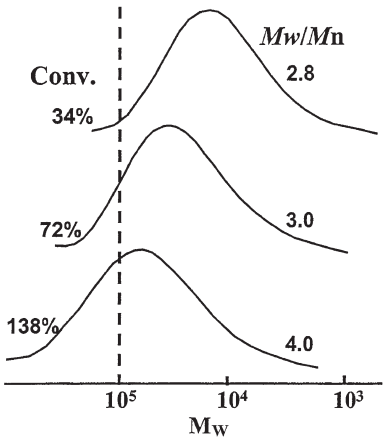

Preparation and Fluorescent Property of Eu(TTA)$_3$Phen Incorporated in Polycarbonate Resin

S. ZHAO, L. ZHANG, W. LI, and L. LI

[Regular Article]
Vol. 38, No. 6, pp 523–526 (2006)

Rare earth complex Eu(TTA)$_3$Phen was synthesized with a new method. The strong fluorescence and high thermal stability of Eu(TTA)$_3$Phen were used for modification of resin. The fluorescence spectra showed that the prepared Eu(TTA)$_3$Phen-PC composite materials retained the fluorescent characteristic and strong red emission of Eu^{3+} complex and its fluorescence intensity was found to be increased with increase in the mass fraction of Eu(TTA)$_3$Phen in PC resin.

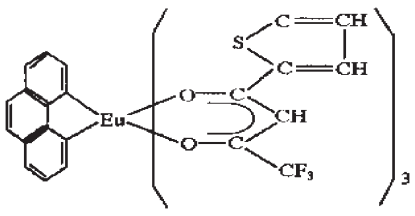

Thermosensitive PNIPA-Based Organic–Inorganic Hydrogels

M. LUTECKI, B. STRACHOTOVÁ, M. UCHMAN, J. BRUS, J. PLEŠTIL, M. ŠLOUF, A. STRACHOTA, and L. MATĚJKA

[Regular Article]
Vol. 38, No. 6, pp 527–541 (2006)

Thermosensitive organic–inorganic hydrogels were prepared by introducing an inorganic phase into the poly(*N*-isopropylacrylamide) (PNIPA) gels. Tetramethoxysilane (TMOS) or [3-(methacryloyloxy)propyl]trimethoxysilane (MPTMOS) were used to form silica or silsesquioxane domains by the sol-gel process *in situ* within the organic matrix. The presence of the inorganic phase, dispersed in the PNIPA gels or covalently attached to the organic polymer, leads to faster swelling-deswelling kinetics and better mechanical properties of the organic–inorganic hydrogels.

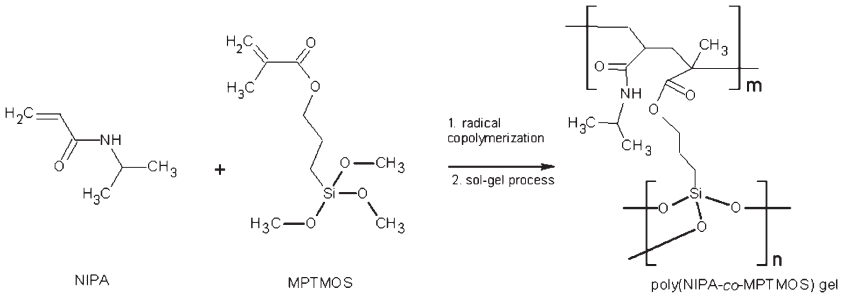

Role of Amorphous Region on the Deformation Behavior of Crystalline Polymers

M. FUKUOKA, T. AYA, H. SAITO, S. ICHIHARA, and H. SANO

[Regular Article]
Vol. 38, No. 6, pp 542–547 (2006)

The yield stress and Young's modulus decreased by extracting the petroleum resin dissolved in the interlamellar amorphous region of HDPE/petroleum resin blends. The TEM observation for the stretched specimen revealed that the decrease of the overall stress is ascribed to the enhancement of the lamellar separation associating with large void formation and lamellar deflection due to the low number density of tie chains which act as a transmitter of the external force.

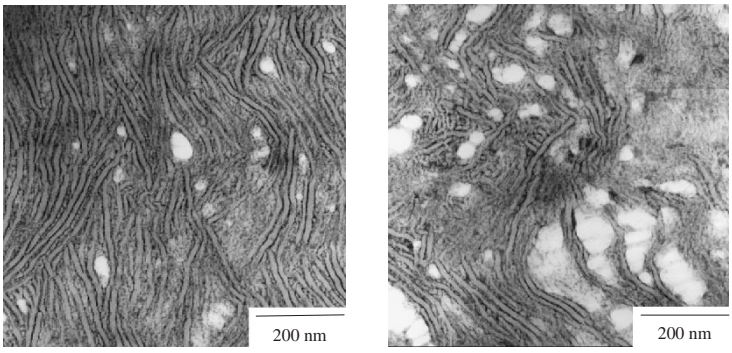

(a) neat HDPE (b) extracted 80/20 HDPE / petroleum resin

TEM micrographs of HDPE lamellae stretched at a stretching rate of λ=2.

Novel Contamination and Gas Sensor Materials from Amphiphilic Polymer-Grafted Carbon Black

H. MOROHASHI, T. NAKANOYA, H. IWATA, T. YAMAUCHI, and N. TSUBOKAWA

[Regular Article]
Vol. 38, No. 6, pp 548–553 (2006)

The responses of electric resistance of composites prepared from amphiphilic polymer-grafted carbon blacks to contamination in solution and solvent vapor were investigated. The electric resistance of the composites from amphiphilic polymer-grafted carbon blacks drastically increased, when it was dipped in *n*-hexane containing contaminations and returned immediately to the initial resistance when it was transferred into dry air. The response of electric resistance of the composite from PNIPAM-grafted carbon black was found to be linearly proportional to chloroform as contamination in *n*-hexane solution and relative humidity.

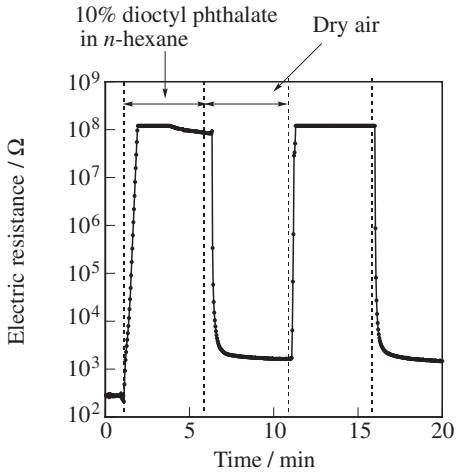

Assembly, Morphology and Thermal Stability of Polyamide 6 Nanotubes

J.-J. LI, G.-J. SONG, X.-L. SHE, P. HAN, Z. PENG, and D. CHEN

[Regular Article]
Vol. 38, No. 6, pp 554–558 (2006)

PA6 nanotubes array has been prepared successfully using small pore anodic aluminum oxide as a template *via* polymer solution and melt wetting method. And the morphology of PA6 nanotubes was highly influenced both by the concentration and the quantity of polymer solution. And its thermal properties were characterized by thermal gravity analysis.

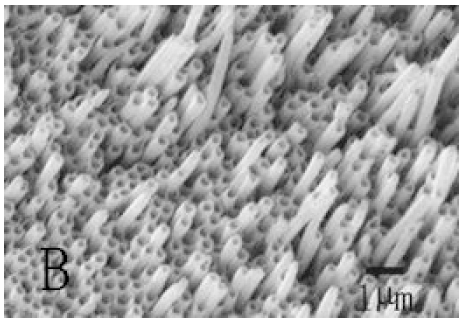

Temperature Dependence of Crystallization Behavior in a Phase-Separated Blend of Poly(*ε*-caprolactone) Homopolymer and Poly(*ε*-caprolactone)-*block*-Polybutadiene Copolymer

M. AKABA and S. NOJIMA

[Regular Article]
Vol. 38, No. 6, pp 559–566 (2006)

The crystallization behavior in a macroscopically phase-separated blend consisting of poly(*ε*-caprolactone) homopolymer (PCL) and PCL-*block*-polybutadiene copolymer (PCL-*b*-PB) is investigated by synchrotron small-angle X-ray scattering (SR-SAXS) and polarized optical microscope (POM) as a function of crystallization temperature T_c. When the blend with $\xi = 2.5\,\mu m$ (ξ: characteristic size of phase separated structure) is quenched into various T_c, two scattering peaks are observed in the SR-SAXS curve during crystallization, which arise from the crystallized PCL and PCL-*b*-PB regions. The growth rates of these scattering peaks are identical at lower T_c ($\leq 35\,^{\circ}C$), while they deviate gradually with increasing T_c.

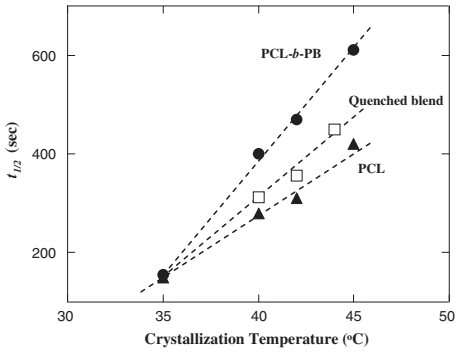

Fabrication of Hierarchically Ordered Hybrid Structures over Multiple Length Scales *via* Direct Etching of Self-Organized Polyhedral Oligomeric Silsesquioxane (POSS) Functionalized Block Copolymer Films

T. HAYAKAWA, M. SEINO, R. GOSEKI, T. HIRAI, R. KIKUCHI, M. KAKIMOTO, M. TOKITA, H. YOKOYAMA, and S. HORIUCHI

[Regular Article]
Vol. 38, No. 6, pp 567–576 (2006)

A novel fabrication of hierarchically ordered organic and inorganic hybrid structures at length scales ranging from nanometers to micrometers was demonstrated by oxygen plasma treatment of self-organized silicon-containing block copolymer films. As a rod-coil type silicon-containing block copolymer, polystyrene-*b*-polyisoprene with polyhedral oligomeric silsesquioxane (POSS) -modified side chains was successfully synthesized. The block copolymer was formed hierarchically structures of hexagonally packed micropores and phase-separated nanodomains *via* self-organization. An oxygen plasma etching to the films provided novel hierarchically ordered hybrid structures.

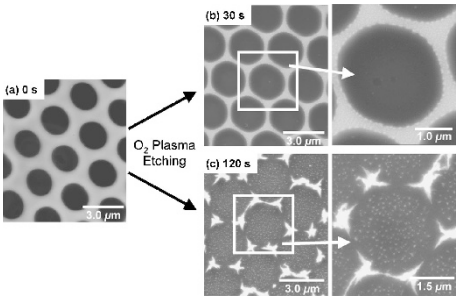

Polymerization of Vinyl Ether by Use of Yttrium Silicate Gel as Solid Acid

O. MORIYA, T. SUGIZAKI, A. KAMEJIMA, K. IWAKURA, T. KUMON, and T. KAGEYAMA

[Regular Article]
Vol. 38, No. 6, pp 577–584 (2006)

The gel of yttrium silicate was found to be an effective solid catalyst for the polymerization of vinyl ethers. The polymerization of ethyl and butyl vinyl ether proceeded readily at 18 °C in the presence of a catalytic amount of the silicate gel, in which the content of yttrium was only 1 mol % to the monomer. When the polymerization of ethyl vinyl ether was carried out in benzene solution, the corresponding polymer was obtained quantitatively irrespective of the concentration of the monomer.

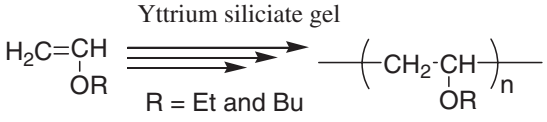

Polymer Structure of Lignophenol I —Structure and Function of Fractionated Lignophenol—

K. MIKAME and M. FUNAOKA

[Regular Article]
Vol. 38, No. 6, pp 585–591 (2006)

A polymer structure and function of lignophenol was examined by various structural analysis of lignophenols fractionated with preparative SEC. The base unit of lignophenol is 1,1-bis (aryl) propane-2-O-aryl ether unit in all the molecular weight areas by NMR analysis. But the amounts of combined cresol and phenolic hydroxyl groups were increased with decreasing molecular weight of fractionated lignophenols. The protein-adsorbing capacities and thermoplastic property of fractionated lignophenols differed with the molecular weights.

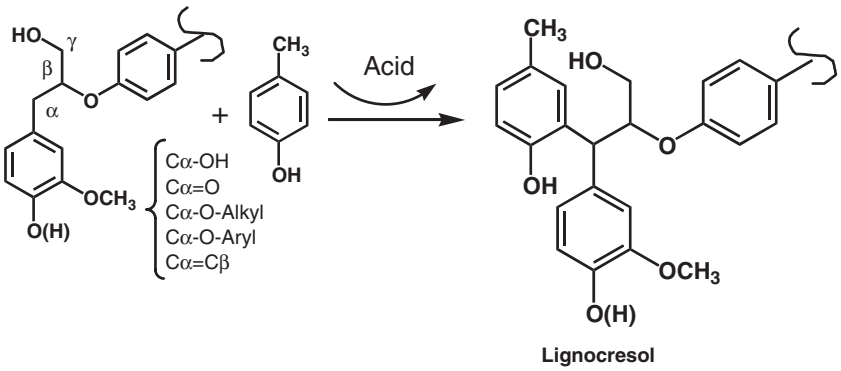

A schematic model of phase separation system.

Polymer Structure of Lignophenol II —Comparison of Molecular Morphology of Lignophenol and Conventional Lignins—

K. MIKAME and M. FUNAOKA

[Regular Article]
Vol. 38, No. 6, pp 592–596 (2006)

The molecular morphology of lignophenol and conventional lignins were analyzed with SEC-MALLS system. The difference in the molecular weight of lignin determined by MALLS and conventional calibration methods using linear polystyrene standard can show the difference of molecular morphology of lignin. The molecular morphology of lignocresol was more spreading and linearity, compared with other lignins. It was suggested that this characteristic of lignophenol is concerned with thermoplasticity of lignophenol that other lignins do not have.

Table I Molecular weights of fractionated lignocresol spruce by SEC/MALLS method.

	PS* Mw	MALLS Mw index	MALLS/PS	PS Mw/Mn	MALLS Mw/Mn
Fr-1	66714	630350	9.45	2.57	1.46
Fr-2	28513	88365	3.10	1.62	1.40
Fr-3	9592	22875	2.39	1.34	1.25
Fr-4	4034	9474	2.35	1.20	1.30
Fr-5	2556	8224	3.21	1.44	1.61
Lignocresol	12922	31940	2.47	3.08	1.83

*polystylene standard method

The EB-DNA Liquid Crystalline Complex with High Concentration of Mg^{2+}

B. LIAO, B. HE, S. CHEN, and Y. HUANG

[Regular Article]
Vol. 38, No. 6, pp 597–602 (2006)

The DNA liquid crystal complexed with ethidium bromide (EB) in the high ionic strength of Mg^{2+} were investigated. It was found that the cholesteric pitch and the fraction of liquid crystal phase in the EB-DNA solution is obviously affected by EB with the same ionic strength of Mg^{2+} at room temperature. The intercalation of EB changes the ionic environment close to the DNA chains and the stiffness of DNA, which affects the liquid crystal behavior of DNA.

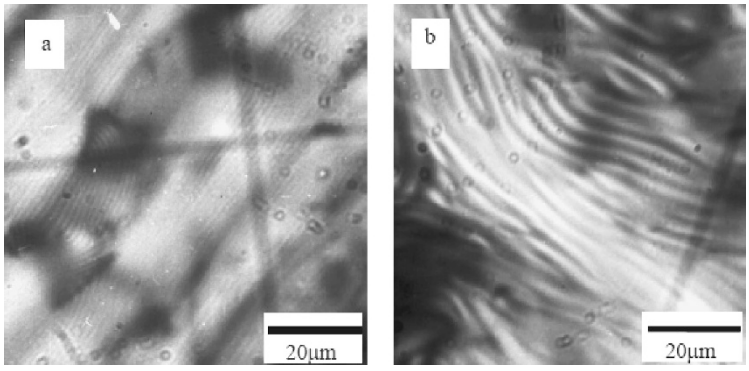

Elasticity of Sphere-forming Polystyrene-*b*-polyisoprene-*b*-poly(2-vinylpyridine)/ Polystyrene-*b*-polyisoprene/Polyisoprene-*b*-poly(2-vinylpyridine) blends: The role of Dangling Chains

Y. TAKAHASHI, Y. AKAZAWA, A. TAKANO, and Y. MATSUSHITA

[Note]

Vol. 38, No. 6, pp 603–605 (2006)

Effects of the dangling ends on the elasticity of sphere-forming ABC tirblock copolymer are examined by addition of AB and BC diblock copolymers. The Young's moduli are proportional to the bridge fraction of middle blocks and the difference between dangling ends and loops are very minor.

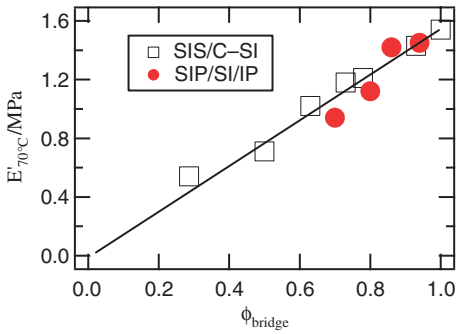

Preparation of Organic/Inorganic Polymer Hybrid from a New Class of Novolac

T. KIMURA, Y. NAKAMOTO, and G. KONISHI

[Note]

Vol. 38, No. 6, pp 606–609 (2006)

The preparation of an organic/inorganic polymer hybrid from a new class of novolac is described. The hybrid was prepared by the acid-catalyzed sol–gel reaction of phenyltrimethoxysilane (PhTMOS) in the presence of anisole novolac. The resulting film was transparent and showed a high heat stability. The dispersion of two components might be due to the utilization of the π–π interaction between the phenyl ring of the silica matrix and that of novolac. This makes it possible to prepare a hybrid glass having a highly content of novolac derivatives.